Role of the amino and carboxy termini in isoform-specific sodium channel variation

Annie Lee and Alan L. Goldin

Department of Microbiology and Molecular Genetics, University of California, Irvine, CA 92697-4025, USA

$Na_v1.2$ and $Na_v1.6$ are two voltage-gated sodium channel isoforms found in adult CNS neurons. These isoforms differ in their electrophysiological properties, even though the major regions that are known to be involved in channel activation and inactivation are conserved between them. To determine if the terminal domains of these channels contributed to their activation and fast inactivation differences, we constructed chimeras between the two isoforms and characterized their electrophysiological properties. Exchanging the N-terminal 205 amino acids of $Na_v1.6$ and the corresponding 202 amino acids of $Na_v1.2$ completely swapped the $V_{½}$ of steady-state activation between the $Na_v1.2$ and $Na_v1.6$ channels in an isoform-specific manner. Exchanging the C-terminal 436 amino acids of $Na_v1.6$ and the corresponding region of $Na_v1.2$ altered the voltage dependence and kinetics of steady-state inactivation, but the changes did not reflect a direct transfer of inactivation properties between the two isoforms. Finally, the N- and C-terminal domains from $Na_v1.6$ demonstrated functional cooperation. These results suggest that the terminal sequences of the sodium channel are important for isoform-specific differences between the channels.

(Received 5 May 2008; accepted after revision 18 June 2008; first published online 19 June 2008)
Corresponding author A. L. Goldin: Department of Microbiology and Molecular Genetics, University of California, Irvine, CA 92697-4025, USA. Email: agoldin@uci.edu

Voltage-gated sodium channels are transmembrane proteins responsible for controlling the influx of sodium currents that depolarize the membrane of neuronal cells. Nine different mammalian voltage-gated sodium channels have been identified (Goldin *et al.* 2000). These channels share a basic structure but differ in their electrophysiological properties, toxin sensitivity, and tissue expression (Goldin, 2001). A voltage-gated sodium channel comprises a pore-forming α subunit and one or more modulatory β subunits in some tissues (Hartshorne & Catterall, 1984). The α subunit alone is sufficient to produce a functional channel (Noda *et al.* 1986), but the properties of the channel can be modulated by the β subunits (Isom *et al.* 1992, 1995). In mammals, there are nine α subunit isoforms ($Na_v1.1$ through $Na_v1.9$) and four β subunit isoforms ($\beta1$ through $\beta4$) (Goldin, 2001; Yu *et al.* 2003).

Many structural features that contribute to the function of the sodium channel α subunit have been identified. The α subunit contains four homologous domains, with each subdivided into six transmembrane helices (Fig. 1*A*). In the cell membrane, the four domains assemble around a central pore through which sodium ions pass selectively (Catterall, 2000). The fourth segment of each domain contains positively charged residues at every third position (Stühmer *et al.* 1989). These 'voltage sensors' are highly conserved across isoforms, and they respond to potential changes with outward movements that trigger pore opening. Activation is quickly followed by inactivation, in which a conserved intracellular linker between domains III and IV blocks the pore (West *et al.* 1992; Patton *et al.* 1992).

The $Na_v1.2$ and $Na_v1.6$ channels are two voltage-gated sodium channel isoforms found in adult CNS neurons. These isoforms differ in their electrophysiological properties, even though they share 75% sequence identity and 84% sequence conservation (Smith *et al.* 1998). The major regions involved in channel activation and inactivation such as the S4 voltage sensor segments, the III–IV linker inactivation particle, and the inactivation particle docking site are conserved between them. Therefore, other regions of the channel most likely confer isoform specificity.

The terminal domains of the channels may be important for the functional differences between these isoforms. The C-terminus can modulate inactivation of $Na_v1.5$ and $Na_v1.8$ (Cormier *et al.* 2002; Motoike *et al.* 2004; Choi *et al.* 2004; Glaaser *et al.* 2006). The C-terminus of $Na_v1.2$ has been shown to affect the kinetics and voltage dependence of steady-state inactivation (Mantegazza *et al.* 2001), and the N-terminus of $Na_v1.2$ may interact with intracellular elements that contribute to the voltage dependence of

 DOI: 10.1113/jphysiol.2008.156299

inactivation (Kamiya *et al.* 2004). In this report, we constructed chimeric channels to study the functional effects of the terminal domains of $Na_v1.2$ and $Na_v1.6$. Replacing the N-terminal 202 residues of $Na_v1.2$ with the corresponding region from $Na_v1.6$ conferred the donor channel's voltage dependence of activation on the host channel. Exchanging the C-terminal 436 amino acids of $Na_v1.6$ and the corresponding region of $Na_v1.2$ altered the voltage dependence and kinetics of inactivation, but the changes did not reflect a direct transfer of inactivation properties between the two isoforms. Finally, the N- and C-terminal domains from $Na_v1.6$ demonstrated functional cooperation that was isoform specific.

Methods

Ethical approval

All experiments were performed according to guidelines established by and with the approval of the Institutional Animal Care and Use Committee of the University of California, Irvine.

Construction of chimeric channels

The $Na_v1.2$-FLAG construct was previously characterized (Smith & Goldin, 1997). Briefly, the *Scn2a* cDNA encoding the rat $Na_v1.2$ channel was tagged at the 5′ end with the synthetic *FLAG* sequence 5′-GACTATAA-AGACGATGACGATAAA-3′. The tagged construct was placed between a cytomegalovirus (CMV) promoter and a polyadenylation signal from the β-globin gene. A T7 promoter was included behind the CMV promoter to facilitate *in vitro* transcription. The cDNA clones encoding the $\beta1$ subunit and $\beta2$ subunit were also previously described (Smith *et al.* 1998).

The *Scn8a* cDNA encoding the mouse $Na_v1.6$ channel was tagged with the *c-myc* sequence 5′-GAGCAAAA-GCTCATCTCAGAAGAGGATCTA-3′ at the 5′ end and placed into the MCS of the mammalian vector pRC/CMV(A) behind a T7 promoter. This $Na_v1.6$ clone differed from the previously published sequence (Burgess *et al.* 1995) in the following places: V5L, K15R, I142T, N153T, E937Q, V958A, and the I–II linker. The E937Q mutation made the channel resistant to tetrodotoxin. The I–II linker in this clone contained 333 amino acids and represented the major splice variant found in rat (Dietrich *et al.* 1998; Smith & Goldin, 1998). The V5L, K15R, I142T and N153T mutations could be restored to wild-type residues with no significant change to the channel's voltage dependence of activation and inactivation or its inactivation kinetics. The effect of the V958A substitution was not tested. The *c-myc* tag did not significantly alter the voltage dependence of activation and inactivation or the inactivation kinetics.

Chimeras of $Na_v1.2$ and $Na_v1.6$ were created using unique restriction sites shared between the two constructs described. Because of the limited number of unique sites, the N-terminal chimera included part of domain I and the C-terminal chimera included part of domain IV. To generate the channel chimeras $Na_v1.6$-N2 and $Na_v1.2$-N6, the gene fragment before the *Nde*I restriction site (amino acid positions A202–Y203) from $Na_v1.2$ was exchanged with the corresponding fragment from $Na_v1.6$.

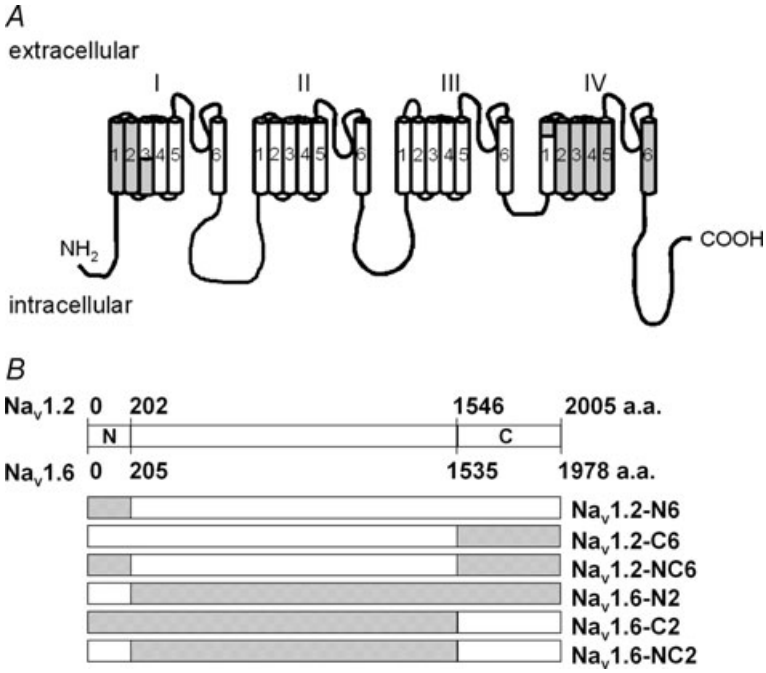

Figure 1. Diagrams of voltage-gated sodium channel and chimeras
A, schematic diagram of the sodium channel indicating the four homologous domains (I–IV), each consisting of six transmembrane segments. The regions that were swapped to construct the chimeric channels are shaded. *B*, the regions swapped between the $Na_v1.2$ and $Na_v1.6$ isoforms are diagrammed for each chimera. Numbers above and below the top bar denote residue positions for $Na_v1.2$ and $Na_v1.6$, respectively. The 'N' region includes the N-terminus and domain I up to the S3 segment. The 'C' region contains domain IV and the C-terminus. Clear bars represent $Na_v1.2$-derived sequences and grey bars represent $Na_v1.6$-derived sequences.

The resulting 'N-region' chimeras switched channel isoform in the third segment of domain I (DIS3). To obtain the chimeras $Na_v1.2$-C6 and $Na_v1.6$-C2, the gene fragment after the *Bst*EII restriction site (amino acid positions M1545–V1546) from $Na_v1.2$ was exchanged with the corresponding fragment from $Na_v1.6$. The resulting 'C-region' chimeras switched channel isoform in the first segment of domain IV (DIVS1). Finally, the double-swap chimeras $Na_v1.2$-NC6 and $Na_v1.6$-NC2 were constructed by exchanging the *Nde*I–*Bst*EII fragments between $Na_v1.2$ and $Na_v1.6$. Figure 1*B* shows the regions exchanged between the $Na_v1.2$ and $Na_v1.6$ α subunits to generate the chimeras. The cDNA construct sequencing was performed by Laguna Scientific (Laguna Niguel, CA, USA).

Expression and electrophysiology

Plasmids containing the channel constructs were linearized at unique restriction sites *Not*I, *Sac*II, or *Sma*I. Capped RNA transcripts were generated from linearized DNA templates using the T7 mMESSAGE mMACHINE transcription kit (Ambion, Austin, TX, USA). RNA yield was estimated by glyoxal gel electrophoresis. Stage V oocytes were removed from adult female *Xenopus laevis* frogs and prepared as previously described (Goldin, 1991). Approximately 0.02–2 ng of RNA was injected per oocyte to obtain current levels between 1 and 5 μA after 24–48 h. Injected oocytes were incubated in ND-96 solution containing 96 mM NaCl, 2 mM KCl, 1.8 mM $CaCl_2$, 1 mM $MgCl_2$, 0.1 mg ml^{-1} gentamicin, 0.55 mg ml^{-1} pyruvate, 0.5 mM theophylline, and 5 mM Hepes at pH 7.5 for 24–72 h at 20°C before analysis.

Sodium currents were recorded from oocytes at room temperature using the two-electrode voltage clamp OC-725 (Warner Instruments, Hamden, CT, USA) with DigiData 1320A interface (Molecular Devices, Sunnyvale, CA, USA) and pCLAMP 8 software (Molecular Devices). Oocytes were maintained in ND-96 solution (without gentamicin, pyruvate and theophylline) during recording. Transient capacitive and leak currents were corrected by *P*/4 subtraction.

The voltage dependence of activation was determined from the sodium currents elicited when the oocyte was step-depolarized from a holding potential of −100 mV to +30 mV in increments of 10 mV. Conductance (G) was calculated using the equation:

$$G = I/(V - V_r),$$

in which I is the current amplitude, V is the test potential, and V_r is the reversal potential. The reversal potential was extrapolated from fitting the I–V curve with the equation

$$I = [1 + \exp(-0.03937z(V - V_{1/2}))]^{-1} g(V - V_r),$$

in which z is the gating charge, $V_{1/2}$ is the half-maximal activity potential, and g is a factor related to the number of channels contributing to the observed current. Conductance values were normalized to the peak conductance and fitted with the two-state Boltzmann equation

$$G = 1/(1 + \exp[-0.03937z(V - V_{1/2})]).$$

The voltage dependence of inactivation was determined from the sodium currents elicited during a −5 mV test pulse immediately after the oocyte was depolarized from a holding potential of −100 mV to a range of conditioning potentials between −95 mV and +25 mV for 100 ms. Currents from the test pulses were normalized to the peak current and fitted with the two-state Boltzmann equation

$$I = 1/[1 + \exp((V - V_{1/2})/a)],$$

in which I is the test pulse current, V is the conditioning potential, $V_{1/2}$ is the half-maximal inactivation potential, and a is the slope factor.

The kinetics of fast inactivation were determined from the inactivation phase of the current traces elicited during the conditioning prepulses in the two-step inactivation protocol. The traces were fitted with the double-exponential equation

$$I = A_{fast} \times \exp[-(t - K)/\tau_{fast}] + A_{slow} \times \exp[-(t - K)/\tau_{slow}] + C,$$

in which I is the current, A_{fast} and A_{slow} are the current fraction inactivating with the time constants τ_{fast} and τ_{slow}, K is the time shift, and C is the steady-state non-inactivating current. The time shift was selected as the point at which the current trace began to inactivate exponentially.

Results

$Na_v1.2$ and $Na_v1.6$ sodium channels show a number of significant differences in their voltage dependence and kinetics of gating, despite the fact that they share 75% sequence identity and 84% sequence conservation (Smith *et al.* 1998). Because the regions that have been identified as the major determinants in channel activation and inactivation are highly conserved between these two channels, differences in other regions of these isoforms are likely to be important in modulating activation and inactivation. To test the hypothesis that the carboxy- and amino-terminal regions are involved in the modulation of gating, we constructed chimeric channels in which those segments were swapped (Fig. 1*B*). The regions that were swapped included the amino terminus up to IS3, which will be referred to as the N-region, and the carboxy terminus plus domain IV, which will be referred to as the

C-region. The chimeras were named based on the parental channel followed by the region that was substituted from the other isoform. For example, $Na_v1.2$-N6 consists of the $Na_v1.2$ channel with the $Na_v1.6$ N-region, $Na_v1.2$-C6 consists of the $Na_v1.2$ channel with the $Na_v1.6$ C-region, and $Na_v1.2$-NC6 consists of the $Na_v1.2$ channel with both N- and C-regions from $Na_v1.6$ (Fig. 1*B*). The reverse chimeras, $Na_v1.6$-N2, $Na_v1.6$-C2 and $Na_v1.6$-NC2, were also constructed. However, we were unable to detect any current through the $Na_v1.6$-NC2 chimera, even though its entire cDNA was sequenced to verify that there were no unintended mutations in the channel that could have prevented its expression. The properties of these chimeric channels were analysed by expression in *Xenopus* oocytes in the absence and presence of the $\beta1$ and $\beta2$ subunits.

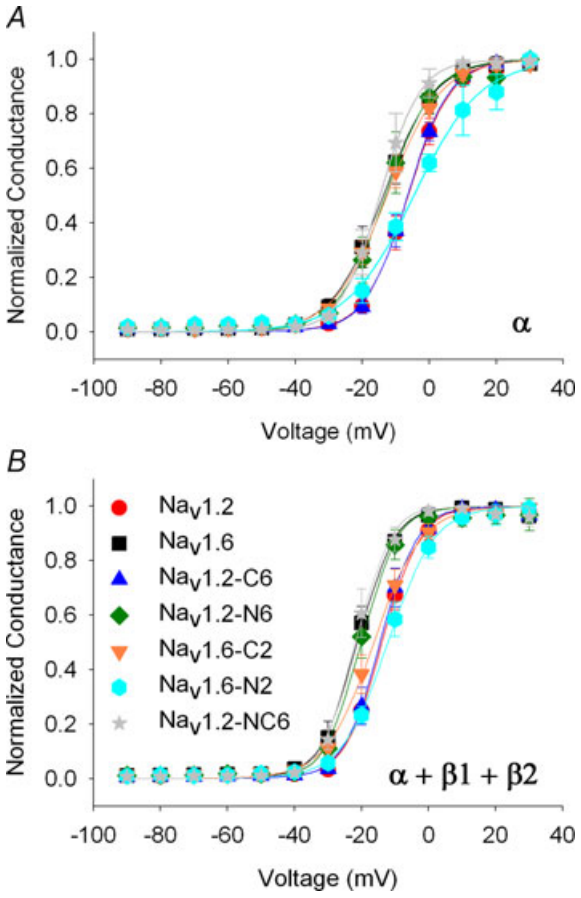

Figure 2. Voltage dependence of activation
Oocytes were injected with RNA encoding each of the parental $Na_v1.2$ and $Na_v1.6$ isoforms and the chimeras as α subunits alone (*A*) or in the presence of $\beta1$ and $\beta2$ subunits (*B*). Sodium currents were recorded by depolarizations from −90 mV to +30 mV in 10 mV increments from a holding potential of −100 mV. Conductance values were calculated by dividing the peak current amplitude by the driving force at each potential and normalizing to the maximum conductance, as described in Methods. The values shown are averages and the error bars are standard deviations. The data were fitted with a two-state Boltzmann equation, and the parameters of the fits are shown in Table 1.

The N-region modulates the voltage dependence of activation

In the absence of the β subunits, $Na_v1.2$ activated at more positive potentials than $Na_v1.6$, with a $V_{½}$ of −6.6 mV for $Na_v1.2$ compared to −14.0 mV for $Na_v1.6$ (Fig. 2*A* and Table 1). Since the S4 voltage sensors are identical in these two isoforms, residues in other regions are most likely responsible for this difference. When the N-region of $Na_v1.2$ was replaced with the corresponding region from $Na_v1.6$ ($Na_v1.2$-N6), the chimera demonstrated a $V_{½}$ of −13.2 mV, which was very similar to that of $Na_v1.6$. In contrast, exchanging the C-region from $Na_v1.6$ into $Na_v1.2$ ($Na_v1.2$-C6) did not significantly affect the $V_{½}$ of activation. Swapping both N- and C-regions from $Na_v1.6$ into $Na_v1.2$ ($Na_v1.2$-NC6) resulted in a channel with a $V_{½}$ for activation of −14.9 mV, which was similar to that of $Na_v1.6$ (Fig. 2*A* and Table 1). These results indicate that the N-terminal 205 amino acids of the $Na_v1.6$ α subunit are important for determining the voltage dependence of activation for this isoform.

To determine if the same region in $Na_v1.2$ was involved in the $Na_v1.2$ voltage dependence of activation, we replaced the N-terminal 205 residues of the $Na_v1.6$ α subunit with the corresponding region from the $Na_v1.2$ isoform ($Na_v1.6$-N2). Unlike our other chimeras, the expression of $Na_v1.6$-N2 in the membrane of *Xenopus* oocytes was very low, even though we injected up to 15 times more RNA compared to the maximum injected for the other chimeras. The cDNA of the entire chimera was sequenced to verify that there were no unintended mutations in the channel that might have decreased expression. On average, we observed 0.2–0.8 μA of current when 2.3–23 ng of RNA were injected, with more variability between oocytes than between the amounts injected. $Na_v1.6$-N2 showed a $V_{½}$ of activation similar to that of $Na_v1.2$ (Fig. 2*A* and Table 1), suggesting that the N-terminal 202 amino acids of the $Na_v1.2$ α subunit were responsible for isoform-specific voltage dependence of activation. Exchanging the C-region from $Na_v1.2$ into $Na_v1.6$ ($Na_v1.6$-C2) resulted in a channel with a $V_{½}$ of activation that was similar to that of the parental $Na_v1.6$ channel, indicating that this region in either channel is not an important determinant of isoform-specific voltage dependence of activation for α subunit channels.

The CNS sodium channel α subunit isoforms normally associate with both $\beta1$ and $\beta2$ auxiliary subunits in 1 : 1 : 1 stoichiometry (Isom *et al.* 1994). Therefore, we examined whether the presence of the β subunits affected the ability of the N-region to convey isoform-specific voltage dependence of activation. The $Na_v1.2$, $Na_v1.6$ and chimeric channels were expressed with at least a 2 : 2 : 1 molar ratio of $\beta1 : \beta2 : \alpha$ subunits, except for $Na_v1.6$-N2, which will be described later. In the presence of $\beta1$ and $\beta2$, the $V_{½}$ of activation was shifted 7.2 mV in the negative

Table 1. Parameters of voltage-dependent activation

	α			$\alpha + \beta1 + \beta2$		
Channel	z (e_0)	$V_{1/2}$ (mV)	n	z (e_0)	$V_{1/2}$ (mV)	n
$Na_v1.2$	4.0 ± 0.1	-6.6 ± 1.6	7	4.6 ± 0.6	-13.8 ± 0.9	5
$Na_v1.6$	3.4 ± 0.3	-14.0 ± 2.6	12	4.7 ± 0.5	-21.6 ± 1.4	3
$Na_v1.2$-N6	3.7 ± 0.4	-13.2 ± 3.1[a]	12	4.8 ± 0.5	-20.4 ± 1.8[c]	4
$Na_v1.2$-C6	4.1 ± 0.2	-6.8 ± 1.4	9	4.8 ± 0.4	-14.7 ± 1.7	11
$Na_v1.2$-NC6	4.5 ± 0.4	-14.9 ± 2.7[a]	11	5.1 ± 0.6	-22.0 ± 1.8[c]	5
$Na_v1.6$-N2	2.6 ± 0.5	-4.5 ± 2.0[b]	3	3.7 ± 0.2	-12.4 ± 1.7[d]	5
$Na_v1.6$-C2	3.2 ± 0.2	-12.9 ± 1.9	9	3.7 ± 0.4	-16.6 ± 1.9[d]	9

[a]Statistically significant difference from $Na_v1.2$ α alone at $P < 0.001$; [b]statistically significant difference from $Na_v1.6$ α alone at $P < 0.001$; [c]statistically significant difference from $Na_v1.2$ $\alpha + \beta1 + \beta2$ at $P < 0.001$; [d]statistically significant difference from $Na_v1.6$ $\alpha + \beta1 + \beta2$ at $P \leq 0.002$.

direction for $Na_v1.2$ and 7.6 mV in the negative direction for $Na_v1.6$, thereby maintaining the voltage difference between the two isoforms (Fig. 2*B* and Table 1). Swapping the N-region from $Na_v1.6$ into $Na_v1.2$ had a similar effect on the voltage dependence of activation in the presence of $\beta1$ and $\beta2$ as it did in their absence, since $Na_v1.2$-N6 showed a $V_{1/2}$ similar to that of $Na_v1.6$ in both cases. $Na_v1.2$-NC6 also maintained the shift to $Na_v1.6$-like voltage dependence in the presence of $\beta1$ and $\beta2$ (Fig. 2*B* and Table 1). These data indicate that the N-region of $Na_v1.6$ also confers isoform-specific voltage dependence of activation in the presence of the β subunits.

Swapping the C-region of $Na_v1.2$ into $Na_v1.6$ ($Na_v1.6$-C2) in the presence of $\beta1$ and $\beta2$ shifted the voltage dependence of activation towards that of $Na_v1.2$ (Fig. 2*B* and Table 1). In contrast, the reciprocal chimera $Na_v1.2$-C6 maintained the voltage dependence of the parental $Na_v1.2$ channel. These results suggest that the difference between $Na_v1.2$ and $Na_v1.6$ in the presence of the β subunits depends at least partially on the C-region.

Because of the low surface expression of $Na_v1.6$-N2, it was necessary to inject large quantities of α subunit RNA to obtain current amplitudes that could be analysed. For this reason, we could not co-inject molar ratios of the β subunits without killing the oocyte, so a 1 : 1 : 2 molar ratio of $\beta1 : \beta2 : \alpha$ was used. Assuming that low expression of $Na_v1.6$-N2 was due to less α subunit protein in the oocyte membrane, then this ratio would still have resulted in a molar excess of protein for the β subunits. In support of this assumption, the current amplitude recorded from coexpression of $Na_v1.6$-N2 and β subunits averaged 2 μA, which was four times the average current amplitude from the same amount of α subunit RNA expressed alone. Furthermore, decreasing the amount of β subunit RNA that was injected to one-tenth the original amount did not decrease the average current amplitude. The increase in current amplitude corresponded well with the current amplitude increase in oocytes shown previously for $Na_v1.2$ α subunits coexpressed with an excess of the β subunits (Isom *et al.* 1992; Isom *et al.* 1995). When $Na_v1.6$-N2 was injected as $\alpha + \beta$ subunits, this chimera demonstrated a $V_{1/2}$ of -12.4 mV, which was similar to that of $Na_v1.2$ coexpressed with the β subunits (Fig. 2*B* and Table 1). Thus, the N-region of $Na_v1.2$ still determined the isoform-specific voltage dependence of activation in the presence of the β subunits.

Both the N- and C-regions affect inactivation

In addition to differences in the voltage dependence of activation, the $Na_v1.2$ and $Na_v1.6$ isoforms showed even larger differences with respect to inactivation. In the absence of the β subunits, $Na_v1.2$ had an inactivation $V_{1/2}$ of -33.8 mV, which was approximately 23 mV more positive than that of $Na_v1.6$ (Fig. 3*A* and Table 2). However, in contrast to their effects on activation, neither the N- nor C-region from $Na_v1.6$ shifted the voltage dependence of inactivation to be comparable to that of $Na_v1.6$ when they were swapped into $Na_v1.2$ individually. Rather, each substitution had a small but statistically significant effect in the opposite direction. Substitution of the N-region ($Na_v1.2$-N6) shifted the $V_{1/2}$ by -4 mV, whereas substitution of the C-region ($Na_v1.2$-C6) shifted it by approximately $+2$ mV. The effects were additive as indicated by the fact that substituting both regions from $Na_v1.6$ into $Na_v1.2$ ($Na_v1.2$-NC6) resulted in a channel with the same inactivation $V_{1/2}$ as $Na_v1.2$ (Fig. 3*A* and Table 2). Substituting the N-region from $Na_v1.2$ into $Na_v1.6$ ($Na_v1.6$-N2) had a larger effect, shifting the $V_{1/2}$ by approximately $+12$ mV towards that of $Na_v1.2$. Substituting the C-region from $Na_v1.2$ into $Na_v1.6$ ($Na_v1.6$-C2) also had a larger effect, shifting the $V_{1/2}$ by approximately -10 mV further away from that of $Na_v1.2$ (Fig. 3*A* and Table 2). Again, neither region could transfer isoform-specific inactivation of $Na_v1.2$ to $Na_v1.6$. These results indicate that the inactivation gating of $Na_v1.6$ is altered to a greater degree than that of $Na_v1.2$ by sequence changes in its terminal regions.

Table 2. Parameters of voltage-dependent inactivation

	α			$\alpha + \beta1 + \beta2$		
Channel	*a* (mV)	$V_{1/2}$ (mV)	*n*	*a* (mV)	$V_{1/2}$ (mV)	*n*
$Na_v1.2$	9.6 ± 0.5	-33.8 ± 0.9	9	8.2 ± 0.7	-47.9 ± 1.6	5
$Na_v1.6$	8.9 ± 0.9	-57.2 ± 2.1	12	6.0 ± 0.3	-53.9 ± 1.6	7
$Na_v1.2$-N6	8.6 ± 0.3	-37.8 ± 2.5[a]	11	7.2 ± 0.2	-47.2 ± 1.0	7
$Na_v1.2$-C6	9.1 ± 0.7	-31.9 ± 1.2[a]	6	7.3 ± 0.5	-43.5 ± 1.6[c]	9
$Na_v1.2$-NC6	8.6 ± 0.4	-34.6 ± 0.8	7	9.0 ± 0.5	-43.0 ± 1.7[c]	5
$Na_v1.6$-N2	12.2 ± 0.8	$-44.3 + 3.3$[b]	4	7.1 ± 0.3	-50.1 ± 0.5[d]	6
$Na_v1.6$-C2	8.0 ± 0.6	-67.1 ± 1.4[b]	9	7.1 ± 0.8	-59.7 ± 1.1[d]	5

[a]Statistically significant difference from $Na_v1.2$ α alone at $P \leq 0.004$; [b]statistically significant difference from $Na_v1.6$ α alone at $P < 0.001$; [c]statistically significant difference from $Na_v1.2$ $\alpha + \beta1 + \beta2$ at $P \leq 0.002$; [d]statistically significant difference from $Na_v1.6$ $\alpha + \beta1 + \beta2$ at $P < 0.001$.

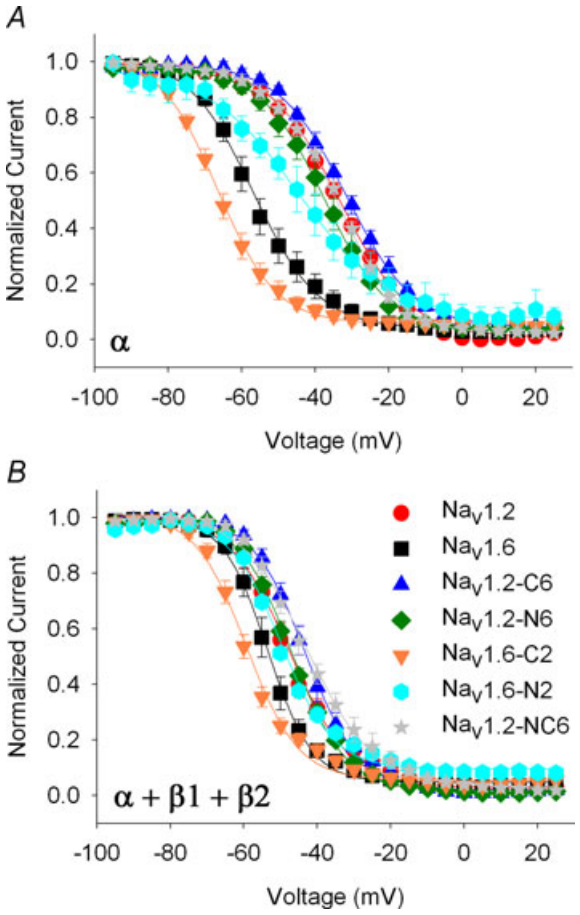

Figure 3. Voltage dependence of inactivation
Oocytes were injected with RNA encoding each of the parental $Na_v1.2$ and $Na_v1.6$ isoforms and the chimeras as α subunits alone (*A*) or in the presence of $\beta1$ and $\beta2$ subunits (*B*). Oocytes were depolarized from a holding potential of −100 mV to a range of conditioning potentials between −95 mV and +25 mV for 100 ms, followed immediately by a test pulse to −5 mV. The peak current amplitude during each test pulse was normalized to the current amplitude of the first test pulse and plotted as a function of the conditioning pulse potential. The values shown are averages and the error bars are standard deviations. The data were fitted with a two-state Boltzmann equation, and the parameters of the fits are shown in Table 2.

The presence of $\beta1$ and $\beta2$ had opposite effects on the voltage dependence of inactivation for $Na_v1.2$ and $Na_v1.6$, thus decreasing the difference between the two isoforms. The two accessory subunits shifted the $V_{1/2}$ of $Na_v1.2$ by approximately −14 mV, and they shifted the $V_{1/2}$ for $Na_v1.6$ by approximately +3 mV (Fig. 3*B* and Table 2). Substituting the N-region from $Na_v1.6$ into $Na_v1.2$ ($Na_v1.2$-N6) in the presence of the β subunits did not have a significant effect, whereas substituting the C-region ($Na_v1.2$-C6) caused an approximately +4 mV shift in the voltage dependence of inactivation. Substituting both regions ($Na_v1.2$-NC6) caused an approximately +5 mV shift in the voltage dependence of inactivation (Fig. 3*B* and Table 2). These effects were greater than those observed in the absence of the β subunits. Substituting the N-region from $Na_v1.2$ into $Na_v1.6$ ($Na_v1.6$-N2) in the presence of the β subunits produced a smaller voltage shift (+4 mV) than it did for the α subunit alone. Substituting the C-region from $Na_v1.2$ into $Na_v1.6$ ($Na_v1.6$-C2) in the presence of the β subunits also produced a smaller voltage shift (−6 mV) than it did for the α subunit alone (Fig. 3*B* and Table 2). Therefore, the β subunits modulated the effects of the α subunit's N- and C-regions on the $V_{1/2}$ of inactivation.

The $Na_v1.2$ and $Na_v1.6$ channels differed in their kinetics of inactivation, with $Na_v1.6$ being faster. The magnitude of the slow time constant for $Na_v1.6$ was either similar to or smaller than that of $Na_v1.2$ at all potentials (Fig. 4*A*), and the magnitude of the fast time constant for $Na_v1.6$ was smaller than that of $Na_v1.2$ at all potentials (Fig. 4*B*). There was also a significantly larger percentage of $Na_v1.6$ current inactivating with the fast time constant at potentials ≤ -5 mV (Fig. 4*C*). Swapping the N-region of $Na_v1.6$ into $Na_v1.2$ ($Na_v1.2$-N6) did not affect the kinetics of inactivation, but swapping the N-region of $Na_v1.2$ into $Na_v1.6$ ($Na_v1.6$-N2) slowed inactivation kinetics by decreasing the percentage of current inactivating with the fast time constant at all potentials (Fig. 4*C*) and increasing the magnitude of the fast time constant

at negative potentials (Fig. 4*B*). Swapping the C-region had a significant effect on the kinetics of inactivation for both isoforms. Swapping the C-region of $Na_v1.2$ into $Na_v1.6$ ($Na_v1.6$-C2) accelerated inactivation, and swapping the C-region of $Na_v1.6$ into $Na_v1.2$ ($Na_v1.2$-C6) slowed inactivation (Fig. 5). However, each effect resulted from a different alteration. The C-region of $Na_v1.2$ decreased the magnitude of the slow time constant

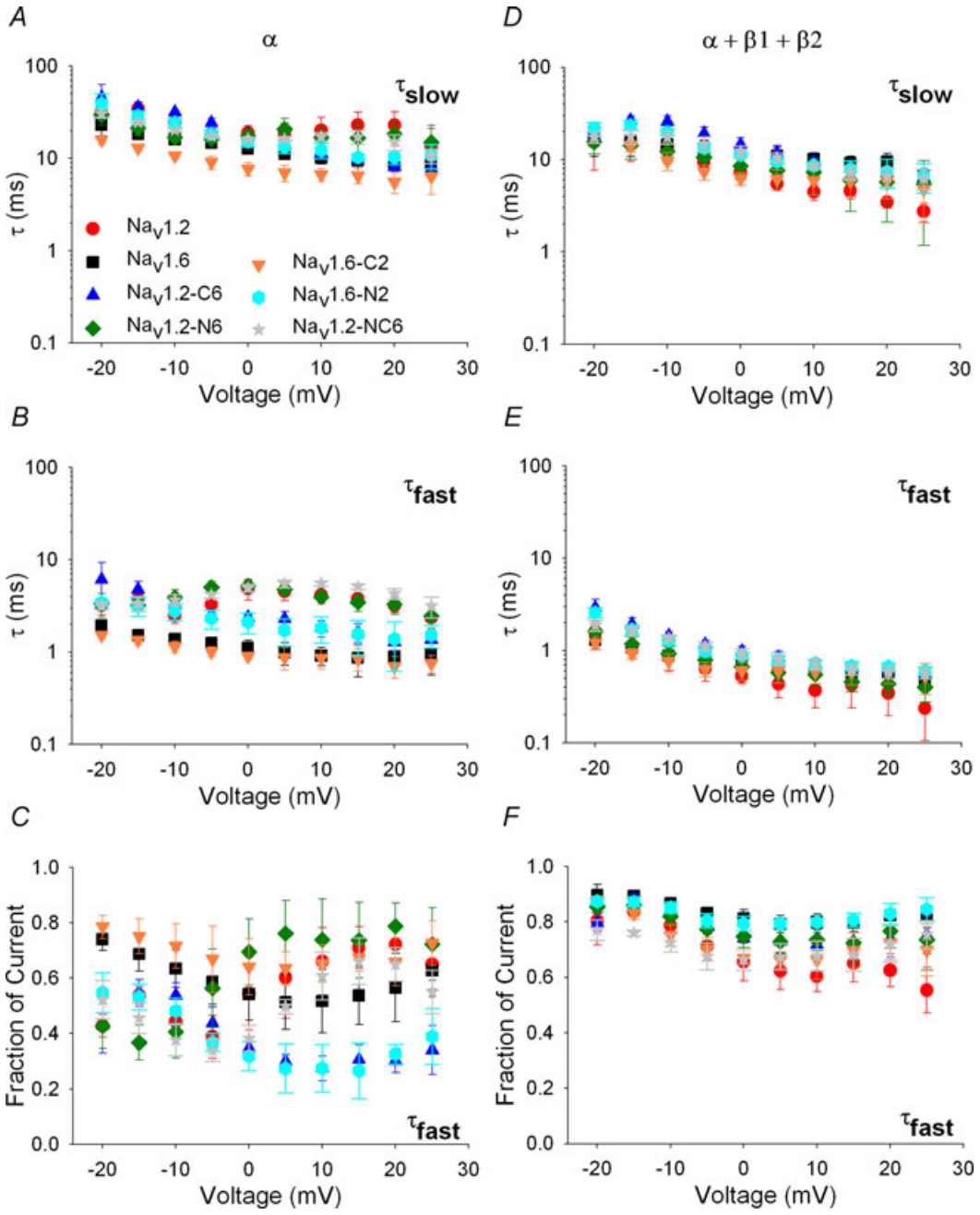

Figure 4. Kinetics of fast inactivation
Oocytes were injected with RNA encoding each of the parental $Na_v1.2$ and $Na_v1.6$ isoforms and the chimeras as α subunits alone (*A*, *B* and *C*) or in the presence of $\beta1$ and $\beta2$ subunits (*D*, *E* and *F*). Traces of sodium currents elicited by 100 ms depolarizations between −25 mV and +20 mV from a holding potential of −100 mV were fitted with the double exponential equation described in Methods. Time constants for the slow component (τ_{slow}) of fast inactivation are plotted on a logarithmic scale in panels *A* and *D*. Time constants for the fast component (τ_{fast}) of fast inactivation are plotted on a logarithmic scale in panels *B* and *E*. Panels *C* and *F* show the fraction of current inactivating with τ_{fast}. The values shown are averages and the error bars indicate standard deviations. Sample sizes were $Na_v1.2$ (8), $Na_v1.6$ (12), $Na_v1.2$-C6 (6), $Na_v1.2$-N6 (9), $Na_v1.6$-C2 (9), Nav1.6-N2 (4), $Na_v1.2$-NC6 (6), $Na_v1.2 + \beta1 + \beta2$ (5), $Na_v1.6 + \beta1 + \beta2$ (7), $Na_v1.2$-C6 $+ \beta1 + \beta2$ (9), $Na_v1.2$-N6 $+ \beta1 + \beta2$ (7), $Na_v1.6$-C2 $+ \beta1 + \beta2$ (5), $Na_v1.6$-N2 $+ \beta1 + \beta2$ (6), $Na_v1.2$-NC6 $+ \beta1 + \beta2$ (5).

compared to $Na_v1.6$ (Fig. 4*A*), while the C-region of $Na_v1.6$ decreased the percentage of current inactivating with the fast time constant at potentials ≥ 0 mV compared to $Na_v1.2$ (Fig. 4*C*). Surprisingly, swapping both the N- and C-regions from $Na_v1.6$ into $Na_v1.2$ ($Na_v1.2$-NC6) restored the inactivation kinetics to be comparable to $Na_v1.2$ (Figs 4*A–C* and 5), even though the N-region by itself had no effect.

Co-expression of the $\beta1$ and $\beta2$ subunits accelerated inactivation of both $Na_v1.2$ and $Na_v1.6$ (compare Fig. 4*D–F* to Fig. 4*A–C*). The β subunits decreased both the slow (Fig. 4*D*) and the fast (Fig. 4*E*) time constants for $Na_v1.2$, but their effect on the percentage of $Na_v1.2$ current inactivating with τ_{fast} was significant only at the negative potentials (Fig. 4*F*). On the other hand, the β subunits substantially increased the percentage of $Na_v1.6$ current inactivating with τ_{fast} at all the potentials examined. The β subunits also altered the fast and slow time constants, although these effects were subtle. In the presence of β subunits, swapping the N-region from $Na_v1.6$ into $Na_v1.2$ ($Na_v1.2$-N6) or the N-region from $Na_v1.2$ into $Na_v1.6$ ($Na_v1.6$-N2) did not have any significant effect (Fig. 4*D–F*). Swapping the C-region of $Na_v1.2$ into $Na_v1.6$ ($Na_v1.6$-C2) lowered the percentage of current inactivating with the fast time constant between -10 and $+10$ mV potentials (Fig. 4*F*). Swapping the C-region from $Na_v1.6$ into $Na_v1.2$ ($Na_v1.2$-C6) slightly increased the magnitudes of the slow and fast time constants (Fig. 4*D* and *E*). Swapping both the N- and C-regions from $Na_v1.6$ into $Na_v1.2$ ($Na_v1.2$-NC6) also slightly increased the slow and fast time constants (Fig. 4*D* and *E*). Overall, swapping the terminal regions in the presence of the β subunits did not cause large shifts in the kinetics of inactivation like the ones associated with swapping the C-region from $Na_v1.6$ into $Na_v1.2$ ($Na_v1.2$-C6) or the N-region from $Na_v1.2$ into $Na_v1.6$ ($Na_v1.6$-N2) in the absence of the β subunits.

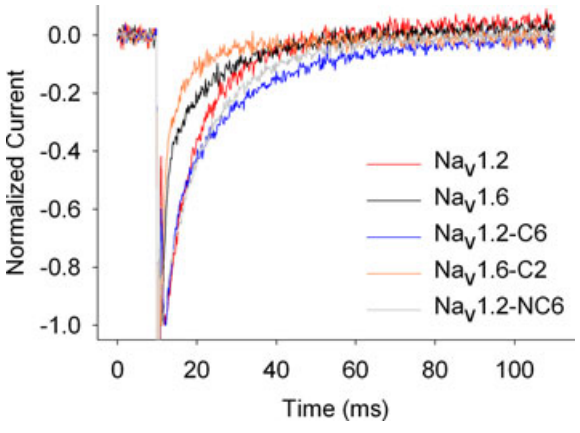

Figure 5. Effects of the C-terminus on inactivation kinetics
Sodium currents were recorded from oocytes expressing parental $Na_v1.2$ and $Na_v1.6$ isoforms and the chimeras as α subunits alone during 100 ms depolarization to 0 mV from a holding potential of -100 mV. Current traces were normalized to directly compare the kinetics of inactivation. The peak current amplitudes were $Na_v1.2$ (1.3 μA), $Na_v1.6$ (1.6 μA), $Na_v1.2$-C6 (1.6 μA), $Na_v1.6$-C2 (1.3 μA), $Na_v1.2$-NC6 (2.2 μA).

Discussion

In this study, we have shown that $Na_v1.2$ has a more depolarized $V_{1/2}$ of activation and a more depolarized $V_{1/2}$ of inactivation than $Na_v1.6$ both in the absence and in the presence of the $\beta1$ and $\beta2$ subunits. These differences are consistent with how the voltage-dependent properties of the two isoforms compare to each other in mammalian neurons in a previous study by Rush *et al.* (2005), suggesting that the comparative voltage-dependent differences between $Na_v1.2$ and $Na_v1.6$ in oocytes reflect their *in vivo* behaviours. We also observed differences between the isoforms in the τ_{slow} of inactivation that were not noted by Rush *et al.* (2005). We further demonstrated that the terminal regions of the $Na_v1.2$ and $Na_v1.6$ α subunits are important for the differences between the two isoforms. The N-region, which includes the N-terminus and the first half of domain I, affects the voltage dependence of activation in an isoform-specific manner. The C-region, which includes domain IV and the C-terminus, influences the voltage dependence and kinetics of inactivation for both isoforms, although it does not confer isoform specificity. Isoform-specific interaction may also be occurring between the N- and C-regions.

Both the N- and C-regions in the chimeras include a portion of a transmembrane domain along with the cytoplasmic terminus. We believe that the cytoplasmic N- and C-termini of $Na_v1.2$ and $Na_v1.6$ are more likely than domains I and IV to be responsible for the differences observed in channel gating because these regions are significantly more divergent than domains I and IV. For example, the domain I S1–S3 regions of $Na_v1.2$ and $Na_v1.6$ are 78.6% identical (94.0% conserved), whereas the N-termini are only 66.1% identical (82.7% conserved). Similarly, the domain IV regions of $Na_v1.2$ and $Na_v1.6$ are 87.2% identical (92.8% conserved), whereas the C-termini are only 65.2% identical (76.4% conserved). However, we cannot rule out the possibility that even conservative substitutions in domain I S1–S3 and domain IV might affect channel gating, based on the recent finding that the mutation I136V shifts the voltage-dependent activation of $Na_v1.7$ (Cheng *et al.* 2008).

Our data indicate that the N-region can shift the $V_{1/2}$ of inactivation as well as impart isoform-specific voltage dependence of activation, suggesting that this region is likely to be involved in the conformational changes coupling activation to inactivation. This hypothesis is supported by changes in the slopes of the activation and

inactivation curves of some N-region chimeras, which might be caused by altered allosteric interactions between the DI–S4 sensor segment responsible for initiating the activation process and the DIV–S4 sensor segment responsible for initiating the inactivation process (Chanda *et al.* 2004). Whether the movements of the S4 segments are affected by isoform-specific N-region differences in the transmembrane segments that alter the packing of S1–S3 around S4 in domain I or by differences in the N-terminus that change its interaction with sites anchoring the S4 segment cannot be determined from our current results.

The C-region can affect both the voltage dependence and kinetics of inactivation. Within this region, the $Na_v1.2$ and $Na_v1.6$ sequences differ the most in the distal halves of their C-termini, which contain 65 residue differences compared to only 19 in the proximal half. Deletions in the distal half of the $Na_v1.2$ C-terminus have been shown to accelerate the inactivation rate and shift the voltage dependence in the negative direction, suggesting that this region inhibits inactivation (Mantegazza *et al.* 2001). It is possible that the C-terminus alters binding of the III–IV linker inactivation particle to the docking site, either by directly interacting with one of these regions or by steric interference. Previous studies have shown that the C-terminus of $Na_v1.5$ modulates inactivation by interacting with the III–IV linker inactivation particle (Cormier *et al.* 2002; Motoike *et al.* 2004; Glaaser *et al.* 2006). Since the C-termini of $Na_v1.2$ and $Na_v1.6$ differ in length and sequence, they may interfere differentially with fast inactivation depending on their proximity to the inactivation gate. However, neither domain IV nor the C-terminus was sufficient to transfer isoform-specific inactivation into $Na_v1.2$ or $Na_v1.6$.

We have also shown that the N-terminal 205 amino acids from $Na_v1.6$ can compensate for the effects of the $Na_v1.6$ C-region. Since the N-region did not affect the inactivation kinetics of $Na_v1.2$ by itself, it is likely that there was cooperativity between the two $Na_v1.6$-derived terminal regions. The possibility that the N-terminus of a voltage-gated sodium channel interacts with another cytoplasmic factor has been suggested for $Na_v1.2$. Kamiya *et al.* (2004) have shown that coexpression of $Na_v1.2$ with its N-terminal 102 amino acid truncation peptide in HEK293 cells can alter the channel's voltage dependence of inactivation. Although we were unable to examine functional cooperation between the N- and C-terminal sequences of $Na_v1.2$ due to difficulties in expressing the $Na_v1.6$-NC2 chimera in *Xenopus* oocytes, our data from the $Na_v1.2$-NC6 chimeric channel suggest that the terminal domains of the $Na_v1.6$ channel isoform do interact.

These results suggest that the C-region of the $Na_v1.6$ sodium channel can interfere with fast inactivation unless the $Na_v1.6$ N-region is present to modulate the influence of the C-region. This modulation may occur through either direct or allosteric interactions between the termini, resulting in movement of the C-terminus away from the inactivation gate. Since this cooperativity did not occur when the terminal regions were from different isoforms ($Na_v1.2$ and $Na_v1.6$), it probably involves molecular determinants in these regions specific to $Na_v1.6$. The interaction is likely to contribute at least partially to the isoform-specific inactivation properties of $Na_v1.6$.

The observation that $Na_v1.6$-N2 showed low expression in oocytes and $Na_v1.6$-NC2 showed no expression suggests that the N-region of $Na_v1.6$ may be important for its stable expression at the surface membrane. The fact that the concomitant loss of the native C-region of $Na_v1.6$ exacerbated the effect of the loss of its native N-region suggests that both regions may contribute to the stability of the channel. We believe that the N-region's effect might reflect the structural folding of the cytoplasmic N-terminus domain. When a soluble fluorescent protein was attached before the N-terminus of $Na_v1.6$-N2, the resulting $Na_v1.6$ N2-ECFP channel had more than twice the average whole-cell current amplitude with 1/25th the amount of RNA injected compared to $Na_v1.6$-N2 (A. Lee & A. L. Goldin, unpublished observations). One possible explanation is that the ectopically placed N-terminus from $Na_v1.2$ misfolded, hindering access to a region that added stability to the protein, and the attachment of the fluorescent protein caused a structural refolding that exposed the site required for stability. We do not know if the N-termini of $Na_v1.2$ and $Na_v1.6$ actually affect channel stability *in vivo*. However, if this region is important for stability *in vivo*, then the surface expression of sodium channels may be regulated by post-translational modification or cofactor binding that alters the tertiary structure of the N-terminus.

Our results show that the $\beta1$ and $\beta2$ subunits influenced the effects of the α subunit N- and C-regions on channel inactivation more than the effects of the N-region on activation. Specifically, the effects of N- or C-region swap on the voltage dependence and kinetics of inactivation were diminished in the presence of the β subunits, suggesting that the regions of the α subunit involved in modulating inactivation were themselves modulated by the β subunits. $Na_v1.6$-N2 was the one chimera that showed an obvious β subunit modulation of its N-region's effect on activation as well as inactivation. $Na_v1.6$-N2 showed distinct slopes for its activation and inactivation curves that were made more similar to the slopes of the other chimeras by the presence of the β subunits. The changes to the slopes of both the activation and inactivation curves might have resulted from changes in allosteric interactions among the voltage sensors. This phenotype, along with the previously noted β subunit enhancement of $Na_v1.6$-N2 functional expression, suggests that the association of β subunits can induce a

global conformational change to the α subunit that affects a wide range of its physiological properties.

References

Burgess DL, Kohrman DC, Galt J, Plummer NW, Jones JM, Spear B & Meisler MH (1995). Mutation of a new sodium channel gene, *Scn8a*, in the mouse mutant 'motor endplate disease'. *Nat Genet* **10**, 461–465.

Catterall WA (2000). From ionic currents to molecular mechanisms: the structure and function of voltage-gated sodium channels. *Neuron* **26**, 13–25.

Chanda B, Asamoah OK & Bezanilla F (2004). Coupling interactions between voltage sensors of the sodium channel as revealed by site-specific measurements. *J Gen Physiol* **123**, 217–230.

Cheng X, Dib-Hajj SD, Tyrrell L & Waxman SG (2008). Mutation I136V alters electrophysiological properties of the $Na_v1.7$ channel in a family with onset of erythromelalgia in the second decade. *Mol Pain* **4**, 1.

Choi J-S, Tyrrell L, Waxman SG & Dib-Hajj SD (2004). Functional role of the C-terminus of voltage-gated sodium channel Nav1.8. *FEBS Lett* **572**, 256–260.

Cormier JW, Rivolta I, Tateyama M, Yang A-S & Kass RS (2002). Secondary structure of the human cardiac Na^+ channel C terminus. Evidence for a role of helical structures in modulation of channel inactivation. *J Biol Chem* **277**, 9233–9241.

Dietrich PS, McGivern JG, Delgado SG, Koch BD, Eglen RM, Hunter JC & Sangameswaran L (1998). Functional analysis of a voltage-gated sodium channel and its splice variant from rat dorsal root ganglion. *J Neurochem* **70**, 2262–2272.

Glaaser IW, Bankston JR, Liu H, Tateyama M & Kass RS (2006). A carboxyl-terminal hydrophobic interface is critical to sodium channel function. Relevance to inherited disorders. *J Biol Chem* **281**, 24015–24023.

Goldin AL (1991). Expression of ion channels by injection of mRNA into *Xenopus* oocytes. *Methods Cell Biol* **36**, 487–509.

Goldin AL (2001). Resurgence of sodium channel research. *Annu Rev Physiol* **63**, 871–894.

Goldin AL, Barchi RL, Caldwell JH, Hofmann F, Howe JR, Hunter JC, Kallen RG, Mandel G, Meisler MH, Berwald-Netter Y, Noda M, Tamkun MM, Waxman SG, Wood JN & Catterall WA (2000). Nomenclature of voltage-gated sodium channels. *Neuron* **28**, 365–368.

Hartshorne RP & Catterall WA (1984). The sodium channel from rat brain – purification and subunit composition. *J Biol Chem* **259**, 1667–1675.

Isom LL, DeJongh KS & Catterall WA (1994). Auxiliary subunits of voltage-gated ion channels. *Neuron* **12**, 1183–1194.

Isom LL, DeJongh KS, Patton DE, Reber BFX, Offord J, Charbonneau H, Walsh K, Goldin AL & Catterall WA (1992). Primary structure and functional expression of the b_1 subunit of the rat brain sodium channel. *Science* **256**, 839–842.

Isom LL, Ragsdale DS, De Jongh KS, Westenbroek RE, Reber BFX, Scheuer T & Catterall WA (1995). Structure and function of the β_2 subunit of brain sodium channels, a transmembrane glycoprotein with a CAM motif. *Cell* **83**, 433–442.

Kamiya K, Kaneda M, Sugawara T, Mazaki E, Okamura N, Montal M, Makita N, Tanaka M, Fukushima K, Fujiwara T, Inoue Y & Yamakawa K (2004). A nonsense mutation of the sodium channel gene *SCN2A* in a patient with intractable epilepsy and mental decline. *J Neurosci* **24**, 2690–2698.

Mantegazza M, Yu FH, Catterall WA & Scheuer T (2001). Role of the C-terminal domain in inactivation of brain and cardiac sodium channels. *Proc Natl Acad Sci U S A* **98**, 15348–15353.

Motoike HK, Liu H, Glaaser IW, Yang A-S, Tateyama M & Kass RS (2004). The Na^+ channel inactivation gate is a molecular complex: a novel role of the COOH-terminal domain. *J Gen Physiol* **123**, 155–165.

Noda M, Ikeda T, Suzuki H, Takeshima H, Takahashi T, Kuno M & Numa S (1986). Expression of functional sodium channels from cloned cDNA. *Nature* **322**, 826–828.

Patton DE, West JW, Catterall WA & Goldin AL (1992). Amino acid residues required for fast sodium channel inactivation. Charge neutralizations and deletions in the III–IV linker. *Proc Natl Acad Sci U S A* **89**, 10905–10909.

Rush AM, Dib-Hajj SD & Waxman SG (2005). Electrophysiological properties of two axonal sodium channels, $Na_v1.2$ and $Na_v1.6$, expressed in mouse spinal sensory neurones. *J Physiol* **564**, 803–815.

Smith RD & Goldin AL (1997). Phosphorylation at a single site in the rat brain sodium channel is necessary and sufficient for current reduction by PKA. *J Neurosci* **17**, 6086–6093.

Smith RD & Goldin AL (1998). Functional analysis of the rat I sodium channel in *Xenopus* oocytes. *J Neurosci* **18**, 811–820.

Smith MR, Smith RD, Plummer NW, Meisler MH & Goldin AL (1998). Functional analysis of the mouse Scn8a sodium channel. *J Neurosci* **18**, 6093–6102.

Stühmer W, Conti F, Suzuki H, Wang X, Noda M, Yahagi N, Kubo H & Numa S (1989). Structural parts involved in activation and inactivation of the sodium channel. *Nature* **339**, 597–603.

West JW, Patton DE, Scheuer T, Wang Y, Goldin AL & Catterall WA (1992). A cluster of hydrophobic amino acid residues required for fast Na^+ channel inactivation. *Proc Natl Acad Sci U S A* **89**, 10910–10914.

Yu FH, Westenbroek RE, Silos-Santiago I, McCormick KA, Lawson D, Ge P, Ferriera H, Lilly J, Distefano PS, Catterall WA, Scheuer T & Curtis R (2003). Sodium channel b4, a new disulfide-linked auxiliary subunit with similarity to β2. *J Neurosci* **23**, 7577–7585.

Acknowledgements

This work was supported by grants from the National Multiple Sclerosis Society (RG3405A) and NIH (NS48336).